Pergamon

Int. J. Solids Structures Vol. 32, No. 10, pp. 1417–1431, 1995

0020–7683/95 $9.50 + .00

0020–7683(94)00192–8

INVERSE BOUNDARY TRACTION RECONSTRUCTION WITH THE BEM

LUCIANO M. BEZERRA and SUNIL SAIGAL
Carnegie Mellon University, Department of Civil Engineering, Pittsburgh, PA 15213, U.S.A.

(*Received* 20 *September* 1993; *in revised form* 20 *July* 1994)

Abstract—A boundary integral formulation is presented for the solution of the inverse elastostatics problem (IESP) of reconstructing missing boundary tractions in two-dimensional structural members. Traction reconstruction may involve the determination of the location of the traction distribution in addition to its extent and amplitude. The missing boundary tractions are rebuilt from measured quantities such as displacements, strains or stresses. These quantities may be obtained from sensors located at some internal or boundary points of the object. The proposed formulation starts with an initial guess for the magnitude, extent and location of the missing boundary tractions and proceeds towards the final traction distribution in a sequence of iterative steps. The inverse problem is written as an optimization problem with the objective function being the sum of the squares of the differences between the measured quantities at each sensor location and the corresponding computed quantities for the assumed boundary traction distribution. The constraints that the missing traction distribution lies within a certain portion of the boundary of the object are imposed. This is done using the step retraction and inverse penalty function approach in which the objective function is augmented by the constraint equations using a penalty parameter. The unknown traction distribution and its location are defined in terms of load and geometric parameters, and the sensitivities with respect to these parameters are obtained in the boundary element framework using the implicit differentiation approach. A series of numerical examples involving the reconstruction of linear, parabolic and trigonometric boundary tractions, respectively, are solved using the present approach. The effect of Gaussian errors in the sensors is also studied. Good reconstruction of the missing boundary tractions is obtained for the examples studied. The advantages of the present boundary element formulation over the corresponding finite element formulations are also outlined.

1. INTRODUCTION

This paper deals with the solution of the inverse elastostatics problem (IESP) of reconstruction of boundary tractions using response measurements from sensors located at discrete, interior or exterior, locations of a solid. Computational techniques for the solution of such problems may provide non-destructive evaluation tools, such as identifying contact regions in neighboring objects, as well as hybrid experimental and numerical methods for the analyses of solids (Weathers *et al.*, 1985; Balas *et al.*, 1983).

In problems of solid mechanics, given sufficient boundary traction and displacement conditions, the displacement, strain and stress fields at any interior point of the body may be obtained from the solution of the boundary value problem. Such problems, with a well-posed set of boundary conditions, are termed direct problems. The existence and uniqueness of the solution for such direct problems has been studied by Sokolnikoff (1956) and Muskhelishvili (1963), among others.

Inverse problems have received attention from the engineering community only in the past few decades. Much of the literature on the solution of inverse problems has been devoted to the area of heat conduction. An extensive survey of such efforts may be found in Beck *et al.* (1985) and Hensel (1991). Other applications of inverse problems in recent years have been, for example, in the areas of geophysics, seismology, image processing (Tikhonov and Goncharsky, 1987), and biomedical engineering (Pilkington, 1982; Rudy and Oster, 1992), to only mention a few. The application of the boundary element method to such a problem was reviewed by Tanaka (1987).

A limited literature exists on the solution of inverse problems in solid mechanics. The IESPs fall under two main categories, namely the reconstruction problems and the identification problems (Baumeister, 1987). In the former, an unknown boundary condition that results in an observed response is determined while in the latter, an unknown portion

of the geometry of the object is determined from a set of given response measurements. The solution of an inverse problem does not necessarily satisfy conditions of existence, uniqueness and stability. A survey of such issues concerning inverse problems may be found in the textbooks by Tikhonov and Arsenin (1977) and Romanov (1987), among others.

The numerical solution of the inverse problems may be obtained using the finite element method (FEM) or the boundary element method (BEM). The significant advantages offered by the BEM for such problems were outlined in Bezerra and Saigal (1991, 1993) where a BEM based formulation for inverse identification problems was also presented. A detailed survey and description of the literature on the solution of inverse identification problems may be found in Tanaka and Masuda (1986), Cruse (1987), and more recently in Tanaka and Bui (1993). The inverse problem of boundary condition reconstruction in elastostatics, despite its numerous physical applications, has received scant attention in the literature so far. Such formulations, for example, may be employed in characterizing tractions at inaccessible regions of critical components in sensitive mechanical equipment. Maniatty *et al.* (1989), Zabaras *et al.* (1989) and Schnur and Zabaras (1990) have used the FEM and the BEM along with the spatial "key-node" regularization procedure for the solution of such problems. These contributions have been presented only recently and deal with the determination of the magnitude of simple distributions of tractions at a given location on the surface of the body. For realistic applications, it is necessary to develop further formulations in order to treat more general traction distributions as well as to include the treatment of unknown regions of the application of these tractions.

In this paper, the IESP of the boundary traction reconstruction is first explained and briefly defined in terms of mathematical equations. The problem is then formulated as a constrained non-linear least-squares optimization problem. A transformation of the constrained optimization problem into an unconstrained one is next carried out. Using function specifications for the unknown boundary tractions and the unconstrained optimization methods, the solution procedure adopted seeks to minimize, in the least-squares sense, the difference between the vector $\hat{\psi}$ consisting of simulated experimental data and the prediction ψ corresponding to a guess of the traction distributions. The geometric constraints that the boundary tractions lie within a certain given portion of the boundary of the solid are imposed, when necessary, by recursively stepping back the search direction length and through the use of penalty functions. The design sensitivities required in the numerical optimization procedure are obtained by the implicit differentiation (Saigal *et al.*, 1989) of the boundary integral equations. A variable metric algorithm (Fox, 1971; Reklaitis *et al.*, 1983) is adopted for the numerical optimization procedure.

A number of examples involving rectangular panels and a rolling arrangement are presented to demonstrate the effectiveness of the present solution procedures in reconstructing boundary tractions. Good solutions were obtained for all cases attempted during this study, including the introduction of small Gaussian errors in the simulated experimental data. It is noted that the present study deals with the determination of: (a) the magnitude and extent of the missing boundary traction data, and (b) the location of the distribution. The latter has not been attempted previously in the literature to the best knowledge of the authors.

2. BOUNDARY TRACTION RECONSTRUCTION

Consider a homogeneous, isotropic, linear elastic, two-dimensional solid Ω, bounded by its boundary Γ, as shown in Fig. 1(a). The direct field problems in elastostatics involve the determination of displacement, strain and stress fields in Ω, provided the following are known (Kubo, 1988): (a) the domain Ω and the boundaries Γ of the solid; (b) the governing equations in the domain; (c) the appropriate boundary conditions on Γ; (d) the material properties involved in the governing equations; (e) the forces or other inputs acting on the solid. Under these conditions the solution may be calculated by a direct analysis using analytical or numerical schemes. If any of the above information is lacking, incomplete, or overdefined, a direct analysis cannot be carried out, and the problem is regarded as an inverse problem.

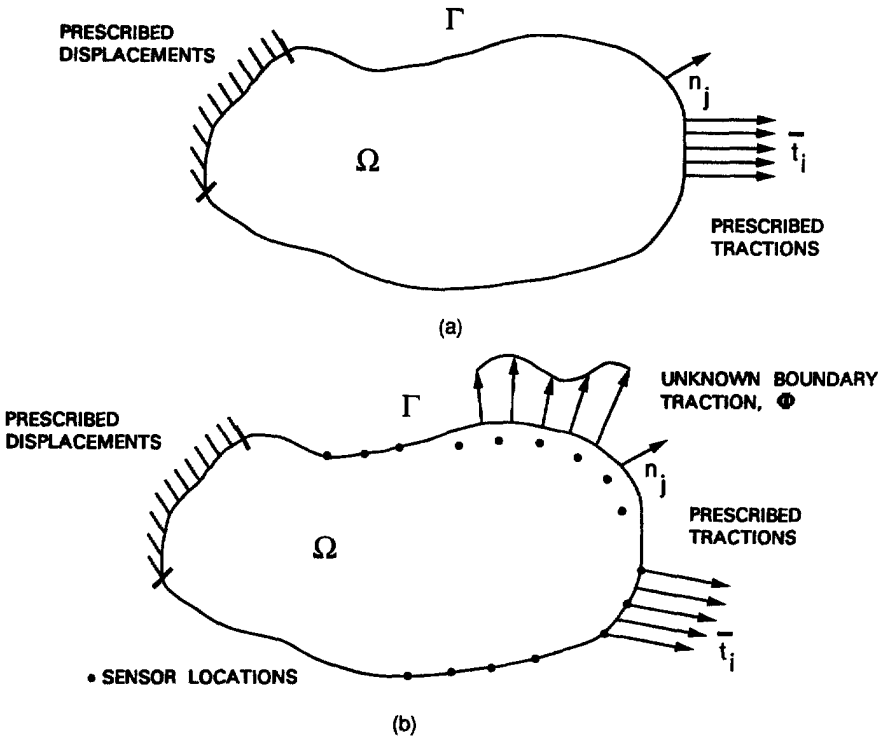

Fig. 1. (a) Direct problem; (b) inverse problem.

The reconstruction of a missing boundary traction, for example Φ in Fig. 1(b), anywhere along the boundary Γ of the solid Ω, constitutes an inverse problem since: (a) the magnitude and the location of the boundary traction are not known; (b) the boundary conditions may be overdefined in that the measured displacement data may be available at a location (degree of freedom) where tractions are already specified; (c) the internal measurement data within the solid Ω may be available as additional information to overcome the lack of sufficient boundary conditions. In mathematical notation, this can be expressed as

$$\sigma_{ij,i}(\mathbf{x}) = -b_j(\mathbf{x}); \quad \mathbf{x} \in \Omega \tag{1}$$

$$\sigma_{ij}(\mathbf{x}) = \lambda \delta_{ij} \varepsilon_{ll}(\mathbf{x}) + 2\mu \varepsilon_{ij}(\mathbf{x}) \tag{2}$$

$$\varepsilon_{ij}(\mathbf{x}) = \tfrac{1}{2}[u_{i,j}(\mathbf{x}) + u_{j,i}(\mathbf{x})] \tag{3}$$

$$\sigma_{ij}(\mathbf{y})\, n_j(\mathbf{y}) = \bar{t}_i; \quad \mathbf{y} \in \Gamma \tag{4}$$

$$u_i(\mathbf{y}) = \bar{u}_i \tag{5}$$

$$\psi_i(\mathbf{v}_k) = \hat{\psi}_{ik}; \quad \mathbf{v}_k \in \Omega \tag{6}$$

where σ_{ij} is the stress tensor; $i,j,l = 1,2$; b_j are the body forces; ε_{ij} is the strain tensor; λ and μ are the Lamé constants; δ_{ij} is the Kronecker delta; n_j denotes the outer normal to the boundary Γ; t_i and u_i are the tractions and displacements, respectively; an overbar ($\bar{}$) denotes prescribed quantities; a hat ($\hat{}$) denotes experimental measurements; ψ_i are the measured displacements, strains, or stresses along direction i at location k ($k = 1,2,3,\ldots,m$); m is the total number of experimental measurements available. In this study, the m observations $\hat{\psi}_{ik}$ may lie inside Ω or on the surface Γ including at locations where tractions are already prescribed, as shown in Fig. 1(b). Equations (1), (2) and (3) denote, respectively, the equilibrium equations, the constitutive relations and the strain–

displacement relations; eqns (4) and (5) denote the traction and displacement boundary conditions, respectively; eqn (6) denotes the measured data.

3. NON-LINEAR LEAST-SQUARES FORMULATION

The vector $\mathbf{z}$ of design variables may be used to completely characterize the magnitude and location of the unknown traction distribution through the mapping $\psi = \mathbf{Az}$, where ψ are the unknown tractions, and $\mathbf{A}$ is a system matrix. The solution of the inverse problem of boundary traction reconstruction involves the determination of the design variables $\mathbf{z}$ such that the quantities ψ match the experimentally measured quantities $\hat{\psi}$ in the least-squares sense. This is accomplished by minimizing the difference between the mapping $\psi = \mathbf{Az}$ and the data vector $\hat{\psi}$ and is expressed as

$$\text{Min}\,[|\,\mathbf{Az} - \hat{\psi}\,|^q]^{1/q}\,;\, q \geqslant 1 \tag{7}$$

where $\mathbf{z}^{\mathrm{T}} = \{z_1, z_2, \ldots, z_n\}$ are the n design variables. The value of q depends upon the type of metric employed in determining the vector norm. The Euclidean norm ($q = 2$) corresponds to least-squares and is commonly employed in minimization problems. It is noted that the least-square norm is not considered to be statistically robust (Scales and Gersztenborn, 1988) unless the data vector $\hat{\psi}$ has errors with a Gaussian probability distribution. The present work is not directed at the study of the error characteristics of experimental measurements and the Euclidean norm is used without further justification. The objective function to be minimized is then written for the two-dimensional case as

$$f(\mathbf{z}) = w \sum_{k=1}^{m} \sum_{i=1}^{2} (\psi_{ik} - \hat{\psi}_{ik})^2 \tag{8}$$

where w is a weighting parameter that is included to enhance the numerical sensitivity in the minimization process; ψ_{ik} are the computed quantities such as displacements, stresses, or strains along direction i and at the location k corresponding to an assumed boundary traction distribution; $\hat{\psi}_{ik}$ are the given experimental measurements.

4. FUNCTION SPECIFICATION FOR TRACTION DISTRIBUTION

In the inverse problem of boundary data reconstruction stated in eqns (1)–(6), it is sought to determine the missing boundary tractions based on a set of given measurements $\hat{\psi}$ at discrete locations within the object or at the boundary of the object. However, due to the ill-posed nature of the problem, a variety of boundary tractions may exist that result in nearly the same measurement data $\hat{\psi}$ in eqn (6) and that result in a local minimization of the objective function given in eqn (8). In addition, small variations in the given data may produce different results unless restrictions on the smoothness of the solution are imposed (Tikhonov and Goncharsky, 1987; Schnur and Zabaras, 1990).

To overcome such instabilities of the inverse problem, *a priori* information on the desired solution is often introduced in the form of smoothness conditions that are implemented through the use of approximating functions or by the regularization of the objective function to be minimized (Tikhonov and Arsenin, 1977; Beck *et al.*, 1985). In the present study, the unknown tractions $\mathbf{\Phi}_j = \sigma_{ij} n_j$ that are required to be reconstructed along the outer normal n_j, are assumed in the form

$$\mathbf{\Phi}_j = \mathbf{\Phi}(\mathbf{z}) = \mathbf{\Phi}_j(\omega, \eta, v) \tag{9}$$

where ω, η and v are a magnitude, a span, and a position that completely define the missing boundary traction using the smooth function $\mathbf{\Phi}_j$. The form of the smooth function $\mathbf{\Phi}_j$, such as linear, parabolic, trigonometric, etc. is assumed to be known.

5. THE MINIMIZATION PROCEDURE

The numerical procedure adopted in this study for the solution of the IESP of boundary traction reconstruction involves the determination of the model vector $\mathbf{z}$ such that the value of the function $f(\mathbf{z})$ in eqn (8) is a minimum. As stated earlier, the model vector $\mathbf{z}$ contains the parameters that completely define the position and the amplitude of the function describing the missing boundary tractions. The possible location of the missing traction is generally limited to a bounded set of locations on the body, say $\bar{\Gamma}_1$. This condition of limiting the location of the missing boundary traction to a feasible geometrical region is expressed in the form of constraint equations as

$$C_j(z_i) \geqslant 0; \quad i = 1,p; \quad j = 1,L \tag{10}$$

where z_i are the components of the vector $\mathbf{z}$; L is the number of geometry constraints; p is the number of design variables used to define the missing boundary tractions. The constraints in eqn (10), together with the minimization of the function in eqn (8), lead to a constrained minimization problem in the theory of optimization.

In the present study, the constrained minimization problem is transformed into an unconstrained minimization problem using the internal penalty function approach (Fox, 1971). Further, the inverse penalty barrier function was employed to represent the geometry constraints. This leads to an augmented objective function of the form

$$F(\mathbf{z}, \mathscr{R}) = f(z) + \theta(C_j(z_i), \mathscr{R}) \tag{11}$$

$$\theta(C_j(z_i), \mathscr{R}) = \mathscr{R} \sum_{j=1}^{L} \sum_{i=1}^{p} \left[\frac{1}{C_j(z_i)} \right] \tag{12}$$

where θ denotes the internal penalty function; C_j are the constraints; $\mathscr{R}$ is an arbitrary penalty parameter; L is the number of constraints; p is the number of design variables in $\mathbf{z}$. It is noted that at the start of the constrained optimization process, a value is assigned to the parameter $\mathscr{R}$, such that the penalty term is of the same order of magnitude as the difference-squared term. As the minimization proceeds, and the missing boundary tractions are closer to the desired solution, the difference term contained in $f(\mathbf{z})$ must play a more prominent role. This is accomplished by reducing the value of the parameter $\mathscr{R}$. The numerical value assigned to $\mathscr{R}$ is problem dependent and an adaptive strategy may be developed to change the value of $\mathscr{R}$ as the minimization progresses. Such an adaptive capability was, however, not developed in the present study. Further discussions on the selection of numerical value for penalty parameters in constrained optimization may be found in, for example, Fox (1971) and Reklaitis *et al.* (1983). The advantages of using the internal penalty function approach as well as the inverse penalty barrier function for inverse problems in elastostatics were discussed in detail in Bezerra and Saigal (1993). The constraints C_j are bounds on the values that $\mathbf{z}$ may assume, and may be expressed as

$$C_j(z_i) = \pm z_i \mp (a \pm \varepsilon) \tag{13}$$

where a is a constant and represents the bounds of the domain and ε is a small number to ensure that the reconstructed traction lies within an $\varepsilon-$neighborhood inside the prescribed portion $\bar{\Gamma}_1$ of the object boundary. For the minimization of the objective function, $F(\mathbf{z}, \mathscr{R})$, given in eqn (11), the variable metric method, which belongs to the quasi-Newton class of optimization methods, was adopted.

6. MINIMIZATION TECHNIQUE

To simplify notation, the function $F(\mathbf{z}, \mathscr{R})$ in eqn (11) is written as $\mathscr{F}(\mathbf{z})$ in the subsequent discussions. The variable metric method is adopted in this paper which postulates that the function $\mathscr{F}(\mathbf{z})$ may be locally approximated, at any iteration n, by a Taylor's

expansion that includes terms up to the quadratic term. Many variations of the variable metric method exist in the literature. The BFGS algorithm has been widely used in the literature (Press *et al.*, 1986; Reklaitis *et al.*, 1983) and has been adopted in this study. For the inverse problem of boundary traction reconstruction, this algorithm starts with an initial guess for the missing tractions defined by the vector $\mathbf{z}^{(0)}$, and generates subsequent updates to this vector according to the following relations:

$$\mathbf{z}^{(n+1)} = \mathbf{z}^{(n)} + \alpha^{(n)} S(\mathbf{z}^{(n)}) \tag{14}$$

$$S(\mathbf{z}^{(n)}) = S^{(n)} = -\mathbf{\Lambda}^{(n)} \mathbf{g}^{(n)} \tag{15}$$

$$\mathbf{g}^{(n)} = \nabla \mathscr{F}(\mathbf{z}^{(n)}) \tag{16}$$

$$\mathbf{\Lambda}^{(n+1)} = \mathbf{\Lambda}^{(n)} - \frac{\mathbf{\Lambda}^{(n)} \Delta \mathbf{z}^{(n)} \Delta \mathbf{g}^{(n)T} \mathbf{\Lambda}^{(n)}}{\Delta \mathbf{z}^{(n)T} \mathbf{\Lambda}^{(n)} \Delta \mathbf{g}^{(n)}} + \frac{\Delta \mathbf{g}^{(n)} \Delta \mathbf{g}^{(n)T}}{\Delta \mathbf{g}^{(n)T} \Delta \mathbf{z}^{(n)}} \tag{17}$$

$$\Delta \mathbf{z}^{(n)} = \mathbf{z}^{(n+1)} - \mathbf{z}^{(n)} \tag{18}$$

$$\Delta \mathbf{g}^{(n)} = \mathbf{g}(\mathbf{z}^{(n+1)}) - \mathbf{g}(\mathbf{z}^{(n)}) \tag{19}$$

where n is the iteration number; $S^{(n)}$ is the search direction; $\alpha^{(n)}$ is the step-length along a line search direction; ∇ is the gradient operator; the sequence $\mathbf{\Lambda}^{(0)}, \mathbf{\Lambda}^{(1)}, \mathbf{\Lambda}^{(2)}, \ldots, \mathbf{\Lambda}^{(n+1)}$ approaches the inverse of the Hessian of the objective function $\mathscr{F}(\mathbf{z})$, starting with $\mathbf{\Lambda}^{(0)} = I$. The above procedure reduces the problem to a uni-dimensional optimization problem of determining the scalar $\alpha^{(n)}$ in eqn (14), that minimizes the objective function along the direction $S^{(n)}$. Given the initial guess $\mathbf{z}^{(0)}$, the derivatives of $\mathscr{F}(\mathbf{z}^{(0)})$ and the search direction $S^{(0)}$ are calculated. Three values of $\alpha^{(n)}$, say $\alpha^{(a)} < \alpha^{(b)} < \alpha^{(c)}$, corresponding to three points $\mathbf{z}^{(a)} < \mathbf{z}^{(b)} < \mathbf{z}^{(c)}$ in eqn (14), along the downhill path of $S^{(0)}$, are found. These points are such that $\mathscr{F}(\mathbf{z}^{(a)}) < \mathscr{F}(\mathbf{z}^{(b)}) < \mathscr{F}(\mathbf{z}^{(c)})$. To ensure that the geometric components of the vector $\mathbf{z}^{(n)}$, say $z_g^{(n)}$, lie inside the feasible boundary domain $\bar{\Gamma}_1$, the step-length $\alpha^{(n)}$ is retracted, when necessary, according to the expression

$$\alpha^{(n)} = \begin{cases} 1.00 \times \alpha^{(n)}; & \text{if } z_g^{(n+1)} \subset \bar{\Gamma}_1 \\ 0.90 \times \alpha^{(n)}; & \text{if } z_g^{(n+1)} \not\subset \bar{\Gamma}_1 \end{cases}. \tag{20}$$

The test in eqn (20) is applied to $\alpha^{(n)}$ repeatedly until $z_g^{(n+1)} \subset \bar{\Gamma}_1$.

Given the three initial feasible points, $\alpha^{(a)} < \alpha^{(b)} < \alpha^{(c)}$, Brent's method (Press *et al.*, 1986) is applied to find the minimum of $\mathscr{F}(\mathbf{z})$ along direction $S^{(0)}$ by approximating the function $\mathscr{F}(\mathbf{z})$ by a parabola fitted through the three points $\{\alpha^{(a)}, \alpha^{(b)}, \alpha^{(c)}\}$. With $\mathscr{F}(\alpha^{(a)}) = \mathscr{F}(\mathbf{z}^{(a)})$, $\mathscr{F}(\alpha^{(b)}) = \mathscr{F}(\mathbf{z}^{(b)})$, and $\mathscr{F}(\alpha^{(c)}) = \mathscr{F}(\mathbf{z}^{(c)})$, solving the inverse interpolation problem, the variable $\alpha^{(m)}$ denoting the minimum of the interpolating parabola is found as

$$\alpha^{(m)} = \alpha^{(b)} + \frac{1}{2} \frac{(\alpha^{(b)} - \alpha^{(a)})^2 [\mathscr{F}(\alpha^{(b)}) - \mathscr{F}(\alpha^{(c)})] - (\alpha^{(b)} - \alpha^{(c)})^2 [\mathscr{F}(\alpha^{(b)}) - \mathscr{F}(\alpha^{(a)})]}{(\alpha^{(b)} - \alpha^{(a)}) [\mathscr{F}(\alpha^{(b)}) - \mathscr{F}(\alpha^{(c)})] - (\alpha^{(b)} - \alpha^{(c)}) [\mathscr{F}(\alpha^{(b)}) - \mathscr{F}(\alpha^{(a)})]}. \tag{21}$$

The above relation fails only if the three points are collinear. Brent's method takes care of this situation by shifting the search for the minimum to the golden section method (Gill *et al.*, 1981) whenever necessary. At the minimum $\alpha^{(m)}$, $\mathscr{F}(\mathbf{z}_m) = \mathscr{F}(\alpha^{(a)})$ is evaluated. The values of $\mathscr{F}(\mathbf{z}^{(a)})$, $\mathscr{F}(\mathbf{z}^{(b)})$ and $\mathscr{F}(\mathbf{z}^{(c)})$ are compared with $\mathscr{F}(\mathbf{z}_m)$ and the one with the most difference is replaced by $\mathscr{F}(\mathbf{z}_m)$. Thus a new triple set of points is obtained. A parabola is fitted through this new set of points, and the process is iteratively applied until the minimum of $\mathscr{F}(\mathbf{z})$, in the search direction being pursued, is found. Upon determining the appropriate $\alpha^{(n)}$ that minimizes $\mathscr{F}(\mathbf{z})$ in the search direction corresponding to iteration n, eqns (17), (14)

and (15) are used to update Λ, S and $\mathbf{z}$, respectively. If convergence has not been achieved, the next iteration then starts with these updated values.

6.1. *Objective function gradient*

The minimization of eqn (11), accomplished by the variable metric algorithm described in the previous section, requires the evaluation of the gradient of the function $\mathscr{F}(\mathbf{z})$ as seen from eqn (16). The gradient of $\mathscr{F}(\mathbf{z})$, with respect to $\mathbf{z}$, may be expressed as

$$\frac{\partial \mathscr{F}}{\partial \mathbf{z}} = 2w \sum_{k=1}^{m} \sum_{i=1}^{2} (\psi_{ik} - \hat{\psi}_{ik}) \frac{\partial \psi}{\partial \mathbf{z}} - \mathscr{R} \sum_{j=1}^{L} \left[\frac{1}{C_j^2(\mathbf{z})} \frac{\partial C_j(\mathbf{z})}{\partial \mathbf{z}} \right] \tag{22}$$

where ψ are the measured quantities and may represent displacements, strains or stresses, respectively; and $\partial\psi/\partial\mathbf{z}$ are the sensitivities of displacements, strains or stresses, respectively, with respect to the parameters $\mathbf{z}$.

The sensitivities $\partial\psi/\partial\mathbf{z}$ are determined in this study using the boundary element method (BEM). The compelling advantages of the BEM for sensitivity analysis have been demonstrated in, among others, Saigal *et al.* (1989). The analytical formulation and numerical implementation considerations for two-dimensional elastostatics sensitivity analysis considered here are available in Saigal *et al.* (1989) and are only briefly discussed below.

The BEM equations, starting from the Somigliana's identity (Banerjee and Butterfield, 1981; Brebbia *et al.*, 1984) for elastostatics and after discretization using interpolation functions, are written in the matrix form as

$$[\mathbf{F}]\{\mathbf{u}\} = [\mathbf{G}]\{\mathbf{t}\} + \{\mathbf{q}\} \tag{23}$$

where $[\mathbf{F}]$ and $[\mathbf{G}]$ are the system matrices; $\{\mathbf{u}\}$ and $\{\mathbf{t}\}$ are the vectors of displacements and tractions, respectively; $\{\mathbf{q}\}$ is the vector of other influences such as body forces, etc. The implicit differentiation of eqn (23) with respect to the design variable $\mathbf{z}$, leads to

$$[\mathbf{F}]\{\mathbf{u}\}_{,z} = [\mathbf{G}]\{\mathbf{t}\}_{,z} + [\mathbf{G}]_{,z}\{\mathbf{t}\} - [\mathbf{F}]_{,z}\{\mathbf{u}\} + \{\mathbf{q}\}_{,z} \tag{24}$$

where the subscript $(,\mathbf{z})$ denotes differentiation with respect to $\mathbf{z}$. The derivations of the matrices $[\mathbf{F}]$ and $[\mathbf{G}]$ and their respective sensitivities, as well as techniques for their numerical evaluations, may be found in, for example, Saigal *et al.* (1989). It is noted that the model vector $\mathbf{z}$ contains parameters that define the location, the distribution, and the magnitude of the missing tractions. The sensitivities $[\mathbf{F}]_{,z}$ and $[\mathbf{G}]_{,z}$ exist only for the components of $\mathbf{z}$ which are related to the location of the missing tractions. These matrix sensitivities vanish for those component of $\mathbf{z}$ that are related to the magnitude of the applied loading. In the latter case the sensitivities of $\{\mathbf{t}\}_{,z}$ in eqn (24) are, however, non-zero.

The sensitivities are obtained by first solving eqn (23) for the unknown displacements and tractions, substituting these quantities in eqn (24), and finally solving eqn (24) for the unknown displacement and traction sensitivities. For the cases where strains and stresses are the measured quantities, the sensitivities of strains and stresses may be obtained from the displacement and traction sensitivities obtained from eqn (24), following the procedure given by Kane and Saigal (1988).

7. EXAMPLES

A number of example problems were considered to evaluate the effectiveness and the limitations of the formulations presented in this paper. In all the examples presented here, the experimental measurements $\hat{\psi}_{ik}$ required in the formulation were obtained from a prior direct BEM analysis with the actual boundary tractions imposed on the structure. These boundary tractions then also served as the "exact" solutions for the purposes of comparison of the accuracy of the present procedures. The "measurement" locations may lie within, or at the boundary of, the object. The measured quantities may be displacements, stresses or

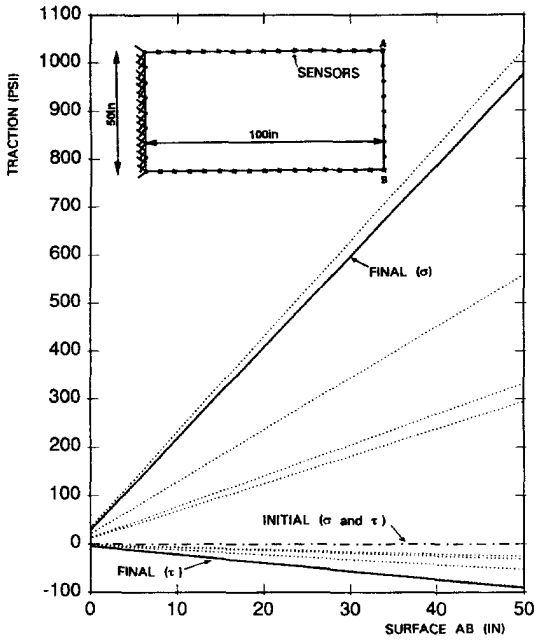

Fig. 2. Linear boundary tractions reconstruction for a rectangular panel.

strains. The algorithm for the minimization of the functional $\mathscr{F}$ in eqn (11) proceeds in an iterative fashion and is considered to have converged when two successive evaluations, $\mathscr{F}_1$ and $\mathscr{F}_2$, of the functional are such that $2\,|\mathscr{F}_1-\mathscr{F}_2| \leqslant \varepsilon \times (|\mathscr{F}_1|+|\mathscr{F}_2|+\bar{\varepsilon})$, where ε is a prescribed tolerance and $\bar{\varepsilon}$ is a small number to account for the special case of converging to exactly zero function value. A value of $\varepsilon = 10^{-3}$ and $\bar{\varepsilon} = 10^{-10}$ was used in the present study. The weighting parameter w was selected such that $wM \gg \varepsilon$, where M is a typical magnitude of the experimental data. In the present study, M ranges in magnitude from 10^{-2} to 10^{3}, and the parameter w was accordingly chosen such that $w \times M \approx 10^{5}$. The penalty parameter $\mathscr{R}$ was varied within an analysis as the iteration proceeded, starting with a large value 10^{5}, subsequently reducing it to 10^{3} and finally to zero. Three-noded quadratic boundary elements were employed for the discretization of the boundary of the object.

7.1. *A rectangular panel under linear tractions*

A rectangular panel shown in Fig. 2 was considered. The geometric dimensions for the panel are shown and the material properties were assumed as modulus of elasticity, $E = 18.6 \times 10^{6}$ psi, and Poisson's ratio, $\nu = 0.3$. The panel is fixed at its left edge and its right edge is subjected to: (a) a normal traction of a linear distribution with a magnitude of zero at A and a magnitude of 1000 psi at B, and (b) a shear traction of a linear distribution with a magnitude of zero at A and a magnitude of 100 psi at B. These two tractions were considered to be missing and are desired to be reconstructed. The measured data consisted of the displacements along the orthogonal x and y directions at 32 points located on the boundary of the panel and depicted by cross symbols in Fig. 2. For purposes of reconstruction, the missing tractions are expressed as

$$\sigma(s) = as+b, \quad \tau(s) = cs+d \tag{25}$$

where σ and τ represent the normal and tangential tractions, respectively; s is the distance along the edge AB; a, b, c and d are unknown constants that define the linear traction distributions and constitute the model vector $\mathbf{z}$ for this case. Thus, a simple case is studied in this example for which the location and the distribution of the missing tractions are known and only their magnitudes need to be reconstructed.

Table 1. Summary of numerical results—no error in measurement data

Case number	Material Properties	This study Initial values	NIT	NRE	Final values	Actual values
I	$E = 1.86 \times 10^6$ psi	$a = 0.0$			975.80	1000
		$b = 0.10$	11	0	28.34	0
		$c = 0.0$			90.46	100
	$v = 0.30$	$d = 0.10$			4.40	0
II	$E = 1.86 \times 10^6$ psi	$P = 300$			1001.0	1000
		$W = 75$	25	3	19.99	20
	$v = 0.3$	$Z = 50$			71.11	70
III	$E = 1217$ N/mm^2	$N = 50$	12	3	34.97	35
	$v = 0.33$	$\gamma = 10$			8.02	8
IV	$E = 1217$ N/mm^2	$N = 55$			35.13	35
		$T = 5$	26	3	10.08	10
	$v = 0.33$	$\gamma = 10$			7.94	8

NIT = number of iterations, NRE = number of restarts.
Case I: rectangular panel with missing linear tractions.
Case II: rectangular panel with missing normal parabolic tractions.
Case III: roller configuration with missing normal contact tractions.
Case IV: roller configuration with missing normal and tangential contact tractions.

The panel was discretized using 30 quadratic boundary elements and 60 nodal points. The initial guess for σ and τ was taken to be a constant traction of 0.1 psi. Thus $a = c = 0$, and $b = d = 0.1$ psi were assumed as the initial guess. Since the location of the traction distribution was fixed, the penalty parameter $\mathscr{R}$ was set to zero for this case. Figure 2 shows the evolution of the missing traction distribution starting from the initial guess. The results for this analysis were also summarized in Table 1 under case I. A good agreement with the exact solution was obtained for both the normal and the tangential traction distributions.

7.2. *A rectangular panel under parabolic tractions*

A simply supported panel, shown in Fig. 3, was considered next. The panel has the same geometry and material properties as those considered in the previous example. The panel is subjected to a normal stress with a parabolic distribution at its top edge. The location Z of the parabolic distribution, the span W of the parabola, and the peak magnitude P of the parabola are unknown and are desired to be reconstructed. The normal distribution may be expressed as

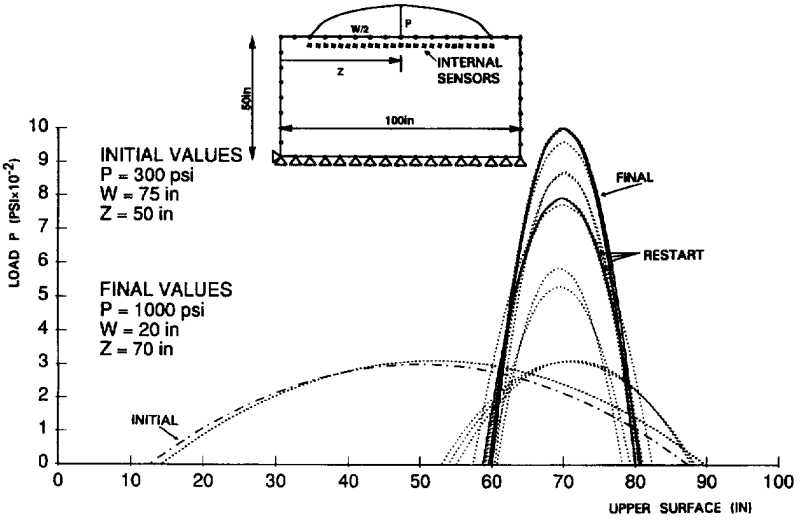

Fig. 3. Parabolic traction distribution reconstruction for a rectangular panel; magnitude (P), span(W) and location (Z).

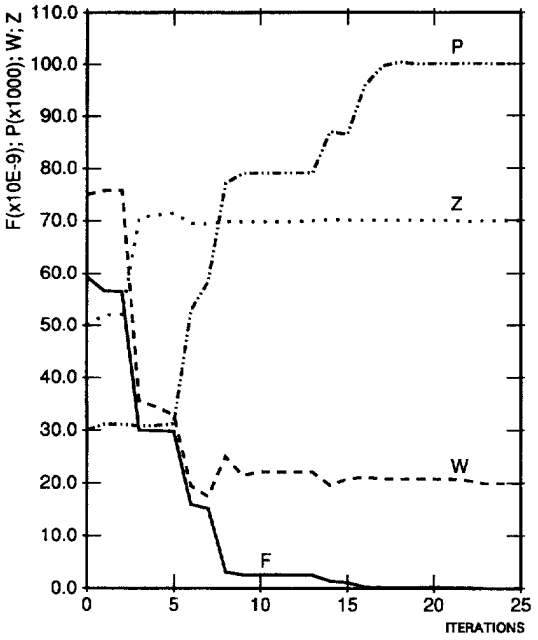

Fig. 4. Convergence of the objective function (F) and the parameters (P, W, Z) defining the missing parabolic boundary tractions.

$$\sigma(s) = -\frac{4P}{W^2}s^2 + \frac{8PZ}{W^2}s + P - \frac{4PZ^2}{W^2} \tag{26}$$

where s is the distance along the span of the parabola, and $(Z-0.5W) \leqslant s \leqslant (Z+0.5W)$. The measured data consists of stresses along the orthogonal x and y directions at 39 locations within the body. These locations are shown by cross symbols in Fig. 3. The parameters P, W and Z constitute the model vector $\mathbf{z}$ for the present case. The initial guess for these parameters was selected as $P = 300$ psi, $W = 75$ in and $Z = 50$ in. The evolution of the missing traction distribution, starting from this initial distribution, as the iterations in the present analysis proceed, is shown in Fig. 3. The exact traction distribution for this case is also shown in bold line in Fig. 3 for comparison and a good agreement is observed. The initial data, the exact data, and other data related to this analysis are given in Table 1 under case II.

As the missing tractions varied in position and span length after each iteration, the BEM mesh for the upper boundary edge was modified to accommodate such evolutions. The penalty parameter $\mathscr{R}$ in eqn (11) was varied during the analysis, changing from a value of 10^5 at the beginning to zero at the end. The convergence history of the traction parameters, as well as of the objective function in eqn (11), are shown in Fig. 4. The final solution was obtained in 25 iterations. The discontinuities in the convergence plots in Fig. 4 correspond to changes of search directions in the optimization process or to changes in the value of the penalty parameter $\mathscr{R}$ during restarts.

The present example deals with the determination of the missing location of the traction distribution in addition to its span and magnitude. Previous analyses reported in the literature have only considered the determination of the magnitude of missing boundary data besides being based on the finite element method (Maniatty *et al.* 1989; Schnur and Zabaras, 1990). The present analysis thus represents an extension over the presently available capabilities for the reconstruction of boundary data.

7.3. *A roller configuration under normal stresses*

The normal tractions acting on a roller at its interface with the workpiece are analysed. The geometry of the roller is given in Fig. 5(a). The inner and the outer diameter of the roller are 10 mm and 89 mm, respectively. The material data for the roller was assumed as

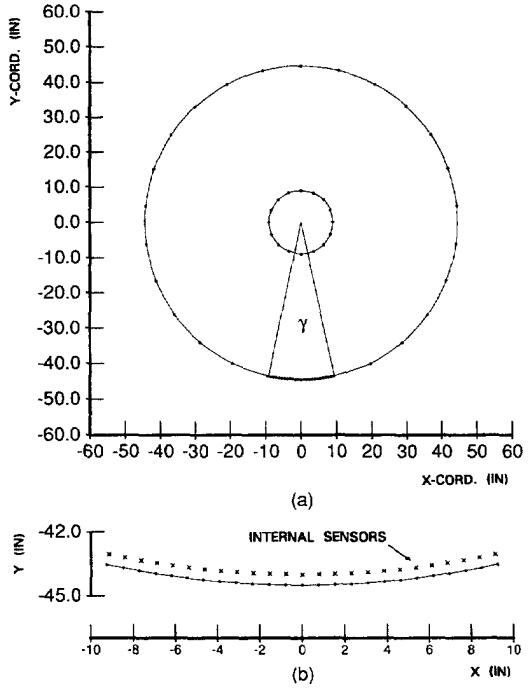

Fig. 5. (a) Roller geometry and discretization; (b) measurement locations.

modulus of elasticity, $E = 1217$ N/mm^2 and Poisson's ratio, $\nu = 0.33$. The roller was discretized using 32 boundary elements with 24 elements on the outer boundary and eight elements on the inner boundary. The boundary region coming in contact with the workpiece and for which the normal tractions are to be reconstructed was discretized using a finer mesh. The measurements were obtained at 25 internal locations identified by solid crosses in Fig. 5(b). The contact region is characterized by angle γ as shown in Fig. 5(a). The normal tractions on this region are assumed to have a sinusoidal distribution and are given as

$$N(\kappa) = A \sin[\kappa\gamma] \tag{27}$$

where N is the normal traction, A is the amplitude of the sinusoidal distribution, and $0 \leqslant \kappa \leqslant 1$. Thus A and γ are the undetermined traction parameters that constitute the model vector **z**. It is noted that this roller configuration has previously been experimentally studied by Theocaris *et al.* (1983). They observed that the normal traction distribution was slightly nonsymmetrical even with a symmetric roller. For simplicity the normal traction distribution is assumed to be symmetric in the present study. The inverse problem defined above has been analysed previously by Schnur and Zabaras (1990) using a finite element formulation and a spatial regularization scheme.

The present example was studied for two sets of measured data at the same internal locations. The first data consisted of displacement measurements while the second data consisted of strain measurements. A contour plot of the function to be minimized in each case was shown in Fig. 6. It is clearly observed from these plots that while a distinct minimum exists for the function corresponding to the strain measurements, a minimum corresponding to the displacement measurements does not exist. Thus, the present formulation can be gainfully used in non-destructive evaluations of components to aid in identifying the measurements that must be made to allow an effective reconstruction of the missing data.

The present analysis was started with an initial guess of $A = 50$ N/mm^2 and $\gamma = 10^\circ$. The evolution of this initial guess towards the final exact distribution in the iterative analysis used in this study is shown in Fig. 7. The key data for this example are also summarized in

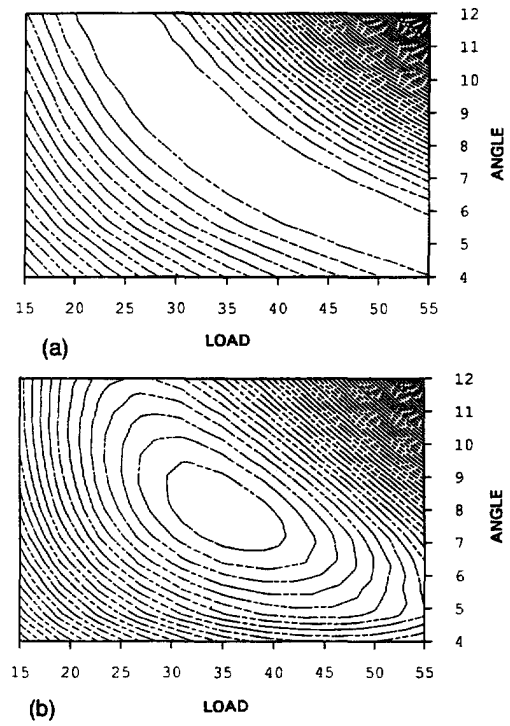

Fig. 6. (a) 50 function contours, 25 displacement sensors; (b) 50 function contours, 25 strain sensors.

Table 1 under case III. The results further demonstrate the capability of the present developments to accurately reconstruct the missing boundary tractions.

7.4. *A roller configuration under sinusoidal normal and tangential stresses*

An extension of the example configuration of the previous section is studied next. In addition to the normal traction distribution, it is desired to reconstruct the tangential traction distribution also. In the experimental observations reported in Theocaris *et al.* (1983), the normal and the tangential tractions were found to be nearly symmetric and antisymmetric, respectively. Based on this observations, the traction distributions may be expressed as

$$N(\kappa) = A \sin[\kappa\gamma], \quad T(\kappa) = B \sin[(\kappa - 0.5)\gamma] \tag{28}$$

where N and T represent the normal and tangential tractions, respectively, and A and B are the amplitudes of the corresponding sinusoidal distributions assumed for each. The

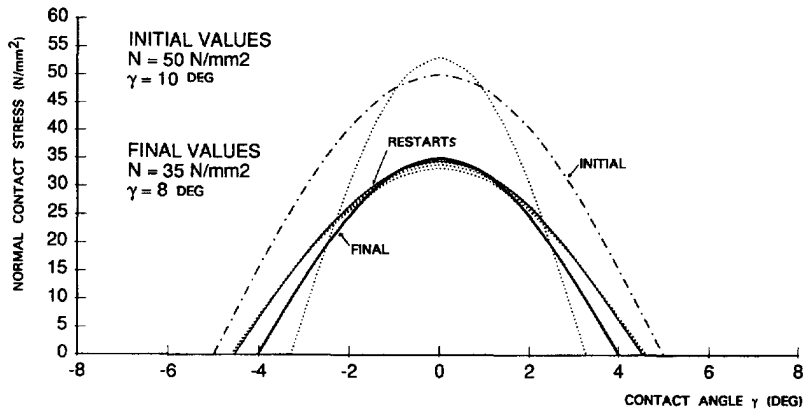

Fig. 7. Evolution of the normal contact stress: two variables.

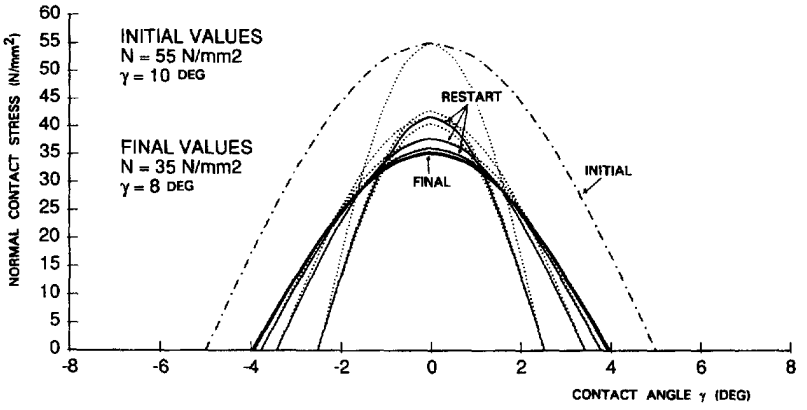

Fig. 8. Evolution of the normal contact stress: three variables.

parameters A, B and γ then define the missing traction distributions and thus constitute the model vector $\mathbf{z}$ for this case. Starting with an initial guess of $A = 55$ N/mm^2, $B = 5$ N/mm^2 and $\gamma = 10°$, the evolution of the normal and the tangential traction distributions were shown in Figs 8 and 9, respectively. The various data for this case are summarized in Table 1 under case IV. It is seen that the present three-parameter problem requires approximately twice the number of iterations required in the previous two-parameter problem for the same geometry configuration. A good agreement of the predictions for missing boundary tractions with the exact solution is also observed. An interesting application of the present example may be the study of the variation of the coefficient of friction along the contact length as the contact pressure varies along the length.

7.5. *Effect of error in the measured data*

A proposed numerical procedure for the solution of inverse problems must be robust in that it should allow prediction of the missing data in the presence of small errors in experimental observations. The analysis of case II for the determination of parabolic normal traction distribution from experimental data observed at 39 stress sensors located within the body was repeated for varying levels of errors introduced into the experimental data. Normally distributed random numbers were added to the experimental data to simulate experimental errors. The errors were considered to be uncorrelated, and were assumed to have a mean, $\hat{\mu} = 0$, and a constant variance. The errors for stress in direction i are picked randomly, with a 99% probability, from the interval $(-\hat{\eta}\hat{\delta}_i, +\hat{\eta}\hat{\delta}_i)$, where $\hat{\delta}_i$ is the average of all stresses along i in the stress data set. A higher value of $\hat{\eta}$ corresponds to larger measurement errors. The results were obtained for increasing values of $\hat{\eta}$ and are shown in

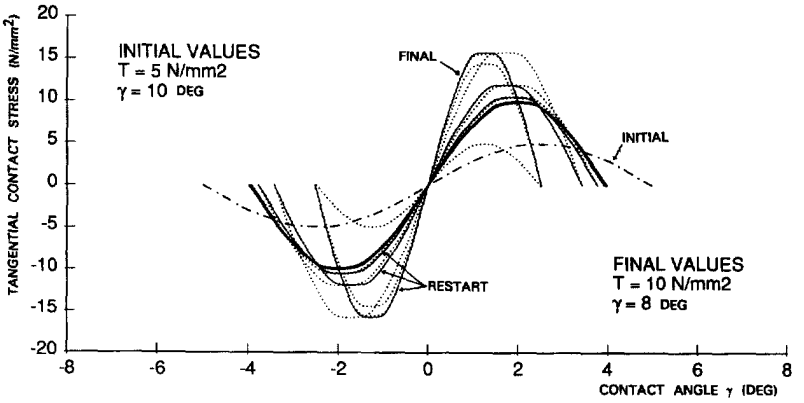

Fig. 9. Evolution of the tangential contact stress: three variables.

Table 2. Effect of small random errors in measurement data

Data error parameter	Standard deviation	Traction N (psi)	Span W (in.)	Position Z (in.)
$\hat{\eta} = 0\%$	$\hat{\sigma} = 0.00$	1000.1	19.99	70.00
$\hat{\eta} = 5\%$	$\hat{\sigma}_1 = 1.38$	1001.1	19.97	71.11
	$\hat{\sigma}_2 = 3.15$			
$\hat{\eta} = 10\%$	$\hat{\sigma}_1 = 2.76$	1001.8	19.94	71.11
	$\hat{\sigma}_2 = 6.31$			
$\hat{\eta} = 15\%$	$\hat{\sigma}_1 = 4.15$	1002.7	19.92	71.11
	$\hat{\sigma}_2 = 9.46$			
$\hat{\eta} = 20\%$	$\hat{\sigma}_1 = 5.52$	1003.6	19.89	71.11
	$\hat{\sigma}_2 = 12.62$			
Exact solution		1000.0	20.00	70.00

$\delta_1 = 71.16$ and $\delta_2 = 162.48$.

Table 2. It is noted from these results that for the example studied, the proposed procedures are quite stable with respect to small errors in the experimental data.

8. CONCLUSIONS

An optimization based integral formulation has been presented for the solution of inverse problems in elastostatics that involve the reconstruction of missing or inaccessible boundary data. The objective function used for the minimization in the optimization procedure was taken to be the square of the difference between a set of experimental measurements and their corresponding computed quantities. The computations are based on an initial guess in the first step and on the refinements of this guess produced by the numerical optimization algorithm in the subsequent steps. A distribution (such as parabolic, sinusoidal, etc.) is assumed for the unknown data and its location, extent of spread, and amplitude are determined by the inverse formulation developed here. The objective function may be augmented by geometric constraints restricting the unknown data to within a prescribed portion of the boundary. The inverse penalty function approach is adopted to transform the constrained problem into an unconstrained one and the minimization is performed using a variable metric method. The response sensitivities required in this algorithm are computed by an analytical approach by performing the implicit differentiation of the boundary integral equations. Such analytical sensitivities aid in a faster convergence of the iterative procedure. A variety of example problems for reconstructing boundary tractions with linear, parabolic, and trigonometric distributions, respectively, are presented. The actual boundary tractions are closely predicted in each case demonstrating the validity of the present approach. Numerical data is also presented to demonstrate the ability of the present approach to reconstruct boundary data from experimental measurements contaminated with the usual order of experimental errors. A prime limitation of the present developments arises from the fact that the optimization procedure upon which they are based may converge to a local minimum especially for cases for which the initial guess is far away from the actual boundary data. A number of applications including determining the variation of coefficient of friction along a contact region and non-destructive evaluation of components may be efficiently treated using the present developments.

Acknowledgments—Luciano Mendes Bezerra acknowledges the financial support provided by the Brazilian National Research Council, CNPq—Conselho Nacional de Desenvolvimento Científico e Tecnológico, and IPEN—Instituto de Pesquisas Energéticas e Nucleares. The support for Dr Sunil Saigal was provided by the National Science Foundation Presidential Young Investigator Grant No. MSS–9057055.

REFERENCES

Balas, J., Sladek, J. and Drzik, M. (1983). Stress analysis by combination of holographic interferometry and boundary integral method. *Expl Mech.* **23,** 196–202.

Banerjee, P. K. and Butterfield, R. (1981). *Boundary Element Methods in Engineering Science.* McGraw-Hill, London.

Baumeister, J. (1987). *Stable Solution of Inverse Problem*. Friedr. Vieweg, Braunschweig.
Beck, J. V., Blackwell, B. and StClair, Jr, C. R. (1985). *Inverse Heat Conduction—Ill-posed Problems*. Wiley-Interscience, New York.
Bezerra, L. M. and Saigal, S. (1991). Flaw detection in elastostatics with boundary element. 22nd Midwestern Mechanics Conference, University of Missouri, Rolla.
Bezerra, L. M. and Saigal, S. (1993). A boundary element formulation for the inverse elastostatics problem (IESP) of flaw detection. *Int. J. Numer. Meth. Engng* **36,** 2189–2202.
Brebbia, C. A., Telles, J. C. and Wrobel, L. C. (1984). *Boundary Elements Techniques—Theory and Applications in Engineering*. Springer-Verlag, Berlin.
Cruse, T. A. (1987). Advanced boundary element methods. *Proc. IUTAM Symp. Advanced Boundary Element Methods*, San Antonio, TX. Springer-Verlag, Berlin.
Fox, R. L. (1971). *Optimization Method for Engineering Design*. Addison-Wesley, MA.
Gill, P. E., Murray, W. and Wright, M. H. (1981). *Practical Optimization*. Academic Press, London.
Hensel, E. (1991). *Inverse Theory and Applications for Engineers*. Prentice-Hall, Englewood Cliffs, NJ.
Kane, J. H. and Saigal, S. (1988). Design-sensitivity analysis of solids using BEM. *J. Engng Mech.* **114,** 1703–1721.
Kubo, S. (1988). Inverse problems related to the mechanics and fracture of solids and structures. *JSME Int. J.* **31,** 157–166.
Maniatty, A., Zabaras, N. and Stelson, K. (1989). Finite element analysis of some inverse elasticity problems. *J. Engng Mech.* **115,** 1303–1317.
Muskhelishvili. (1963). *Some Basic Problems of The Mathematical Theory of Elasticity*. Noordhoff, The Netherlands.
Pilkington, T. C. (1982). *Engineering Contributions to Biophysical Electrocardiography*. IEEE Press, New York.
Press, W. H., Flannery, B. P., Teukolsky, S. A. and Vetterling, W. T. (1986). *Numerical Recipes*. Cambridge University Press, New York.
Reklaitis, G. V., Ravindran, A. and Ragsdell, K. M. (1983). *Engineering Optimization—Methods and Applications*. John Wiley, New York.
Romanov, V. G. (1987). *Inverse Problems of Mathematical Physics*. VNU Science Press, The Netherlands.
Rudy, Y. and Oster, H. S. (1992). The electrocardiographic inverse problem. *Critical Rev. Biomed. Engng* **20,** 25–45.
Saigal, S., Aithal, R. and Kane, J. H. (1989). Conforming boundary elements in plane elasticity for shape design sensitivity. *Int. J. Numer. Meth. Engng* **28,** 2795–2911.
Scales, J. A. and Gersztenkorn, A. (1988). Robust methods in inverse problems. *Inverse Problems* **4,** 1071–1091.
Schnur, D. S. and Zabaras, N. (1990). Finite element solution of two-dimensional inverse elastic problems using spatial smoothing. *Int. J. Numer. Meth. Engng* **30,** 57–75.
Sokolnikoff, I. S. (1956). *Mathematical Theory of Elasticity*. McGraw-Hill, New York.
Tanaka, M. (1987). Some recent advances in boundary element research for inverse problems. In *Boundary Elements X* (Edited by C. A. Brebbia), Vol. 2, pp. 567–581. Springer-Verlag, Berlin.
Tanaka, M. and Bui, H. D. (1993). Inverse problems in engineering mechanics. *Proc. IUTAM Symp. Inverse Problems in Engineering Mechanics*, Tokyo. Springer-Verlag, Berlin.
Tanaka, M. and Masuda, Y. (1986). Boundary element method applied to some inverse problems. *Engng Anal.* **3,** 138–143.
Theocaris, P. S., Stassinakis, C. A. and Mamalis, A. G. (1983). Roll-pressure distribution and coefficient of friction in hot rolling by caustics. *Int. J. Mech. Sci.* **25,** 833–844.
Tikhonov, A. N. and Arsenin, V. Y. (1977). *Solutions of Ill-posed Problems*. John Wiley, New York.
Tikhonov, A. N. and Goncharsky, A. V. (1987). *Ill-posed Problems in the Natural Sciences*. MIR Publishers, Moscow.
Weathers, J. M., Foster, W. A, Swinson, W. F. and Turner, J. L. (1985). Integration of laser-speckle and finite element techniques of stress analysis. *Expl Mech.* **25,** 60–65.
Zabaras, N., Morellas, V. and Schnur, D. (1989). Spatially regularized solution of inverse elasticity problems using the BEM. *Comm. Appl. Numer. Meth.* **5,** 547–553.